Imaging Through Turbulent Media Using Deep Learning Method

The following publication L. Zhou, X. Chen and W. Chen, "Imaging Through Turbulent Media Using Deep Learning Method," 2020 IEEE 18th International Conference on Industrial Informatics (INDIN), Warwick, United Kingdom, 2020, pp. 521-524 is available at https://doi.org/10.1109/INDIN45582.2020.9442210.

LINA ZHOU
Department of Electronic and Information Engineering,
The Hong Kong Polytechnic University,
Hong Kong, China

XUDONG CHEN
Department of Electrical and Computer Engineering,
National University of Singapore,
Singapore 117583, Singapore

WEN CHEN
Department of Electronic and Information Engineering,
The Hong Kong Polytechnic University,
Hong Kong, China
*Email: owen.chen@polyu.edu.hk

***Abstract*—We present deep learning method that can be used to reconstruct high-quality objects through turbulent media mixed with water and milk. The objects are placed behind turbulent media, and a series of speckle patterns are correspondingly recorded. By using many pairs of the recorded speckle patterns and input object images, a designed convolutional neural network (CNN) is fully trained, and then enables the recorded speckle patterns to be processed in real time. The proposed method is promising for imaging through turbulent media, and it is also believed that the proposed method can be applicable in many areas, e.g., imaging and information optics (such as optical encoding).**

Keywords—deep learning method, optical imaging, turbulent media

I. INTRODUCTION

A number of methods using novel imaging mechanisms or sophisticated devices have been devised to recover the image of a target [1–7]. A precondition for the success of imaging the target is that optical systems should be placed in relatively ideal environments. In fact, it is unlikely to satisfy the demands according to actual environments, leaving a great space for us to seek for new and better ways to bypass these restrictions, e.g., thick scattering media [8], time-consuming calculation [9] and the limited application prospects [10]. Recently, imaging through turbid media becomes one of the most challenging and meaningful topics in optics [11–13]. Its cause of difficulties in imaging through turbid media is that light is scattered when propagating through turbid media. The scattering impedes the delivery of valuable information, resulting in impairment of object resolution or the total corruption of object images [14]. The noise-induced artifacts significantly affect quality of the recovered objects, and correspondingly obstruct the development of imaging technologies.

Over the past many years, seeing through scattering or turbid media has shown its necessity and potential applications in various disciplines associated with imaging, ranging from biology science to macroscopic science [15]. Meanwhile, much research work has been implemented to develop methods to resolve the problem. (i) For thin scattering media and relatively pure liquids, enhancing its contrast by manually adjusting exposure time of the digital camera [16] has been widely applied in some near-infrared spectral regions. This method shows to be superior in simple environments, and is often adopted in practice. However, it fails to recover the images in complex environments. (ii) Time-gated holographic imaging technique has been introduced to record the image of a target [17]. Quality of the images reconstructed from digital holograms was evidently degraded because of the noise aroused by scattering media. (iii) Optical imaging combined with mathematical algorithms was proposed to detect the object through turbid media, however it is not helpful for object recovery in heavy conditions [18]. (iv) Much progress has been made by calculating transmission matrix with a huge amount of data and precise measurements to represent the relationship between the recorded pattern and the object [19]. However, it is limited to its high sensitivity which means that slight perturbations can lead to the entirely different transmission matrix. The aforementioned methods are limited by their narrow ranges of applicability, since they work well in relatively easy environments.

In this paper, the objective is to overcome the inevitable limitations existing in previous methods by imaging the objects through murky water using deep learning. The deep learning [20] is a subfield of machine learning which can discover multiple levels of distributed representations and achieve senior abstractions from data by using the nested hierarchy of specially-treated architectures [21,22]. The proposed approach uses convolutional neural network (CNN) [21] to solve inverse problems in optical imaging in complicated circumstances. Some learning-based methods for object recognition and reconstruction through scattering media (e.g., diffusers and slabs) have been studied [23–28]. However, those methods were usually applicable to thin scattering media, and did not take the robustness into consideration. Here, by training the learning model with sufficient pairs of the object images and the recorded speckle patterns, the objects placed behind murky water can be reconstructed from the recorded speckle patterns.

II. EXPERIMENTAL DEMONSTRATION

Digital holography could fail to recover the object placed behind turbid water. The main reason is that the object beam scattered by turbid media is incoherent with the reference beam, and the recorded speckle pattern is usually an indispensable part for holographic reconstruction on account of the carried information. The prevailing techniques still have a long way to acquire satisfactory reconstruction. The deep learning method proposed here does not have to be confined to those constraints. A schematic optical setup is illustrated in Fig. 1(a). In the experimental setup, a laser beam launched by a He-Ne laser source (Newport R-30993, 633.0 nm and 12 mw) is first expanded after transmitting through a microscope objective (Newport, M-40X, 0.65 NA), and then the expanded light is collimated by a collimating lens (f=50.0 mm). After that, the expanded and collimated laser beam passes through a water tank to illuminate onto spatial light modulator (SLM, Holoeye LC-R 720, reflective). The water tank (100.0 mm in the length, 50.0 mm in the width and 30.0 mm in the height) contains a certain concentration of turbulent media. The

inhomogeneous medium used in this experiment is prepared by a mixture of pure water and milk. The objects used in the experiment are handwritten-digit images (i.e., grayscale images with pixel values ranging from 0 to 255) from MNIST database [29] which is widely used to test machine learning method. Size of the grayscale images is 28×28. The targeted images are sequentially displayed by the SLM using a programmable controller in order to modulate the incident beam [30]. The reflected light from the SLM passing through a linear polarizer makes the SLM act as an amplitude object. Then, the modulated object wave goes through water tank again before being recorded by a camera (Thorlabs DCC3240M) with 1280×1024 pixels and pixel size of 5.30 μm × 5.30 μm. The camera is placed an axial distance away from the water tank, and is placed more axial distances away from the SLM to record speckle patterns. Exposure time of the camera is controlled by the LabView program with the value of 200.0 ms. A typical sample sent to the SLM is shown in Fig. 1(b), and the corresponding speckle pattern recorded by the camera is shown in Fig. 1(c). A window with 100×100 pixels is used to select a region of interest from the recorded speckle pattern in order to reduce the computational load.

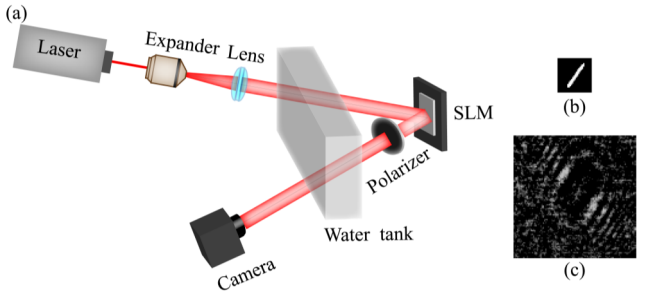

Fig. 1. (a) Experimental setup for imaging through murky water, (b) the object image displayed by the SLM, and (c) a typically recorded speckle pattern.

III. Methodology

The designed CNN-based method consists of two successive steps: training and testing. In the training stage, some pairs of the recorded speckle patterns and the corresponding ground truths (i.e., the object images) are fed to the CNN model as shown in Fig. 2. The designed CNN architecture is described as follows: The input with dimension of 100×100 pixels is the image conditionally recorded by the camera. It convolves with 20 kernels of size 3×3 forming the first convolution layer with size of 96×96×20. The activation function used is the sigmoid function which is frequently applied in machine learning because of its property of boundedness. In the first pooling layer, an action of down-sampling is taken to reduce the computational load to the size of 48×48×20. The pooled data is sent to the second convolution layer which adopts the same number and size of kernels and the same activation function. The second convolve layer has the size of 44×44×20, followed by the second pooling layer with size of 22×22×20. After processing of convolution and down-sampling, the first reshaping layer reshapes the second pooling layer (size of 22×22×20) to a 1×9680 vector and then the vector is transported to the fully connected layer with size of 1×784. Before the last layer of the output image, the second reshaping layer reshapes the 1×784 vector to a 28×28 image which represents the estimation. Finally, the trained CNN model can serve to predict unknown object image from the intensity pattern recorded by the camera. In Fig. 2, a typical prediction from speckle pattern is also shown, i.e., in the testing phase. The CNN architecture is implemented by Matlab2009 on a PC with Nvidia Geforce GTX1080Ti GPU.

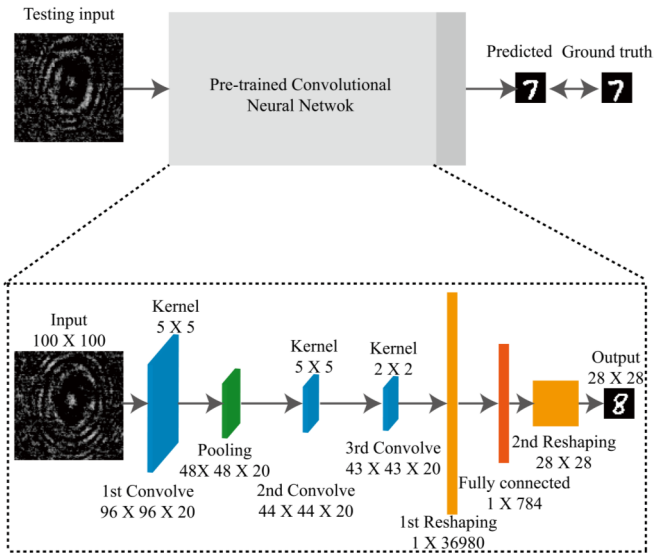

Fig. 2. Schematic of the proposed CNN architecture. Input is cropped from the recorded speckle pattern by using a window with size of 100×100 pixels. Blue blocks represent the convolved processes, and green block indicates the pooling process. The orange bar and plane denote the process of reshaping. The red bar denotes the fully-connected layer.

Here, some pairs of speckle patterns and the ground truths (i.e., the object images) are used in the training phase, and some other pairs are used in the testing phase. The recorded speckle patterns are resized to 100×100 pixels acting as input images for the training, and the dimension of predicted objects is 28×28 pixels as that of the ground truths. In the training and testing, the input speckle pattern is preprocessed by subtracting its mean value to remove the DC component. The loss function used in the designed CNN model is mean squared error (MSE) [31,32], and the optimization function applied to update the weights and biases of the network to minimize the MSE value is stochastic gradient descent (SGD) [33,34]. The updating rule is SGD [33–38]. The velocity for the weight (w) and bias (b) is 0 at the initial stage and then updated by momentum m (-9.5×10^{-5}) and the learning rate α. The weight and bias are updated by the continuously-updated velocity. The weight is initialized to 10^{-3} in the first convolve layer, to be 10^{3} in the second convolve layer and to be 10^{-3} in the fully-connected layer. The initial value of the learning rate is 10^{-6}, and it is accelerated by doubling every 200 inputs sent to the network. The MSE value becomes the smaller when approaching to the optimal value after 5 epochs of iterations in this experiment. The CNN model is trained in 30 minutes, and then the object predictions can be made in real time.

IV. Experimental Results and Discussion

In the first experiment, the trained CNN model is applied to predict the objects placed behind a murky medium mixed by 1200 ml of water and 40 ml of milk. The training dataset and the testing dataset are from MNIST database, i.e., grayscale handwritten-digit images. In the first experiment, the total number of handwritten-digit images chosen from MNIST database and then sent to SLM is 2000, and 2000 speckle patterns are correspondingly recorded by the camera where 1900 pairs of speckle patterns and the corresponding

object images are used in the training phase and another 100 pairs are used in the testing phase. The axial distance from the camera to the water tank is 70.0 mm, and the axial distance between the camera and the SLM is 180.0 mm. Typical examples of the recorded speckle patterns and the predictions made by using the proposed method are shown in the first column and the second column of Fig. 3, respectively. The images in the third column show the ground truths. It can be seen that the speckle patterns are disturbed by the diluted milk. The outputs predicted by using the designed CNN architecture are of high quality, since the recorded speckle patterns contain apparent features to be identified by using the proposed learning method. It is illustrated here that the proposed CNN model performs well in recovering the images of objects placed behind murky water.

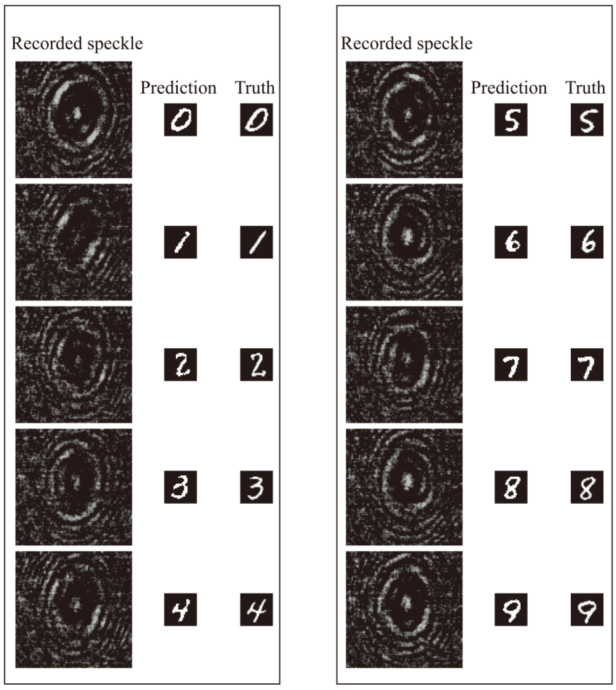

Fig. 3. The CNN-based testing results for object images selected from MNIST database. Typical examples are presented in two blocks. The first column lists the recorded speckle patterns. The second column shows the corresponding predictions made by using the trained CNN model. The third column shows the ground truths (i.e., the object images).

In addition to the prediction of handwritten-digit images selected from MNIST database, the designed CNN model can also perform well in making predictions of object images out of the database. In the second experiment, the optical setup is the same as that used in the first experiment. The 200 totally different images which consist of double-digits, irregular shapes and letters are sent to the SLM, which are not used in the training phase of the designed CNN model. 200 speckle patterns are correspondingly recorded by the camera and sent to the input layer of the trained CNN architecture. The typical results are shown in Fig. 4. The recorded speckle patterns, the reconstructed objects by using the CNN model and original images with the double-digits and the irregular shape are respectively shown at the first three columns. The results for input images with letters are respectively shown at another three columns. It is illustrated in Fig. 4 that the recovered objects are of high quality, and the trained CNN model does have the advantage to predict the totally unknown objects (i.e., not used in the training phase). The above results demonstrate that the designed CNN model provides a solution to reconstruct the object image placed through turbid medium. When the objects are from a different database and are not used during the training, the trained CNN architecture can still offer a feasible scheme to recover the objects.

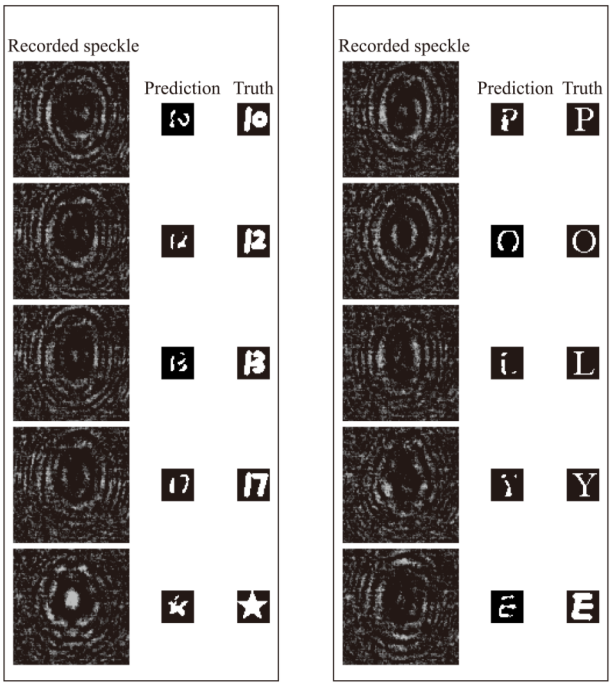

Fig. 4. The CNN-based testing results for object images not from the MNIST database. The typical examples are presented in two blocks. The first column lists the recorded speckle patterns. The second column shows the corresponding predictions made by the trained CNN model. The third column shows ground truths (i.e., the object images).

V. Conclusions

The CNN architecture has been presented for high-quality object reconstruction through turbulent media mixed with water and milk. The trained learning model is validated to have the capability to predict different objects which are not used for the training. The proposed method is promising for various applications, such as imaging through turbid environments and information optics (e.g., optical security).

Acknowledgments

The supports from National Natural Science Foundation of China (NSFC) (61605165), Shenzhen Science and Technology Innovation Commission (JCYJ20160531184426473) and Hong Kong Research Grants Council (25201416, C5011-19G) are acknowledged. Xudong Chen acknowledged the support by the National Research Foundation, Prime Minister's Office, Singapore under its Competitive Research Program (CRP Award No. NRF-CRP15-2015-03).

References

[1] A. P. Mosk, A. Lagendijk, G. Lerosey, and M. Fink, "Controlling waves in space and time for imaging and focusing in complex media," Nature Photon., vol. 6, pp. 283-292, May 2012.

[2] K. Xu, "Current–voltage characteristics and increase in the quantum efficiency of three-terminal gate and avalanche-based silicon LEDs," Appl. Opt., vol. 52, pp. 6669–6675, September 2013.

[3] J. Romberg, "Imaging via Compressive Sampling," IEEE Signal Process. Mag., vol. 25, pp. 14–20, March 2008.

[4] S. R. Arridge and M. Schweiger, “A Gradient Based Optimization Scheme for Optical Tomography,” Opt. Express, vol. 2, pp. 213–225, March 1998.

[5] Y. Wang, Y. Liu, J. Suo, G. Situ, C. Qiao and Q. Dai, “High speed computational ghost imaging via spatial sweeping,” Sci. Rep., vol. 7, pp. 45325, March 2017.

[6] S. C. Park, M. K. Park, and M. G. Kang, “Super-resolution image reconstruction: a technical overview,” IEEE Signal Process., Mag. vol. 20, pp. 21–36, 2003.

[7] M. Duarte, M. Davenport, D. Takhar, J. Laska, T. Sun, K. Kelly, and R. Baraniuk, “Single-pixel imaging via compressive sampling,” IEEE Signal Processing Magazine, vol. 25, pp. 83–91, March 2008.

[8] J. Bertolotti, E. G. van Putten, C. Blum, A. Lagendijk, W. L. Vos, and A. P. Mosk, “Non-invasive imaging through opaque scattering layers,” Nature, vol. 491, pp. 232–234, Novenmber 2012.

[9] M. J. Sun, M. P. Edgar, G. M. Gibson, B. Sun, N. Radwell, R. Lamb, and M. J. Padgett, “Single-pixel three-dimensional imaging with time-based depth resolution,” Nat. Commun., vol. 7, pp. 12010, July 2016.

[10] J. H. Shapiro, “Computational ghost imaging,” Phys. Rev. A, vol. 78, pp. 061802(R), December 2008.

[11] S. M. Popoff, G. Lerosey, M. Fink, A. C. Boccara, and S. Gigan, “Image transmission through an opaque material,” Nat. Commun., vol. 1, pp. 81, September 2010.

[12] O. Katz, E. Small, and Y. Silberberg, “Looking around corners and through thin turbid layers in real time with scattered incoherent light,” Nat. Photonics, vol. 6, pp. 549–553, July (2012).

[13] A. Drémeau, A. Liutkus, D. Martina, O. Katz, C. Schülke, F. Krzakala, S. Gigan, and L. Daudet, “Referenceless measurement of the transmission matrix of a highly scattering material using a DMD and phase retrieval techniques,” Opt. Express, vol. 23, pp. 11898–11911, April 2015.

[14] A. Ishimaru, Wave Propagation and Scattering in Random Media, (Academic Press, Inc., San Diego 1978).

[15] V. Ntziachristos, “Going deeper than microscopy: the optical imaging frontier in biology,” Nat. Methods, vol. 7, pp. 603–614, July 2010.

[16] C. D. Mobley, Light and Water. Radiative Transfer in Natural Waters, (Academic Press, New York, 1994).

[17] A. V. Kanaev, K. P. Judd, P. Lebow, A. T. Watnik, K. M. Novak, and J. R. Lindle, “Holographic imaging through extended scattering media under extreme attenuation,” OSA Imaging Systems, ITu3E, San Francisco CA, June 26–29, 2017.

[18] A. Liutkus, D. Martina, S. Popoff, G. Chardon, O. Katz, G. Lerosey, S. Gigan, L. Daudet, and I. Carron, “Imaging with nature: compressive imaging using a multiply scattering medium,” Sci. Rep., vol. 4, pp. 5552, July 2014.

[19] J. W. Goodman, W. H. Huntley, D. W. Jackson, and M. Lehmann, “Wavefront-reconstruction imaging through random media,” Appl. Phys. Lett., vol. 8, pp. 311–313, November 1966.

[20] Y. LeCun, Y. Bengio, and G. Hinton, “Deep learning,” Nature, vol. 521, pp. 436–444, May 2015.

[21] S. Mallat, “Understanding deep convolutional networks,” Phil. Trans. R. Soc. A, vol. 374, pp. 203, April 2016.

[22] Y. Bengio, A. Courville, and P. Vincent, “Representation learning: A review and new perspectives,” IEEE Trans. Pattern Analysis Machine Intelligence, vol. 35, pp. 1798–1828, August 2013.

[23] R. Horisaki, R. Takagi, and J. Tanida, “Learning-based imaging through scattering media,” Opt. Express, vol. 24, pp. 13738–13743, June 2016.

[24] A. Sinha, J. Lee, S. Li, and G. Barbastathis, “Lensless computational imaging through deep learning,” Optica, vol. 4, pp. 1117-1125, September 2017.

[25] Y. Rivenson, Y. Zhang, H. Günaydın, D. Teng, and A. Ozcan, “Phase recovery and holographic image reconstruction using deep learning in neural networks,” Light Sci. Appl., vol. 7, pp. 17141, October 2017.

[26] S. Li, M. Deng, J. Lee, A. Sina, G. Barbastathis, "Imaging through glass diffusers using densely connected convolutional networks," Optica, vol. 5, pp. 803–813, July 2018.

[27] M. Lyu, W. Wang, H. Wang, H. Wang, G. Li, N. Chen, and G. Situ, “Deep-learning-based ghost imaging,” Sci. Rep., vol. 7, pp. 17865, December 2017.

[28] G. Satat, M. Tancik, O. Gupta, B. Heshmat, and R. Raskar, “Object classification through scattering media with deep learning on time resolved measurement,” Opt. Express, vol. 25, pp. 17466–17479, July 2017.

[29] http://yann.lecun.com/exdb/mnist/

[30] H. Aharoni and M. du Plessis, “The spatial distribution of light from silicon LEDs,” Sensors and Actuators A: Physical, vol. 57, pp. 233–237, December 1996.

[31] Y. Zeng, Y. Fu, M. Bengtsson, X. Chen, W. Lu and H. Ågren, “Finite-difference time-domain simulations of exciton-polariton resonances in quantum-dot arrays,” Opt. Express, vol. 16, pp. 4507–4519, March 2008.

[32] K. Xu, “Monolithically integrated Si gate-controlled light-emitting device: science and properties,” J. Opt., vol. 20, pp. 024014, January 2018.

[33] L. Bottou, “Large-scale machine learning with stochastic gradient descent,” In Proceedings of COMPSTAT'2010 Physica-Verlag HD, pp. 177–186, September 2010.

[34] L.N. Zhou, Y. Xiao, and W. Chen, “Imaging through turbid media with vague concentrations based on cosine similarity and convolutional neural network,” IEEE Photon. J., vol. 11, pp. 7801315, August 2019.

[35] L.N. Zhou, Y. Xiao, and W. Chen, “Machine-learning attacks on interference-based optical encryption: experimental demonstration,” Opt. Express, vol. 27, pp. 26143-26154, September 2019.

[36] L.N. Zhou, Y. Xiao, and W. Chen, “Vulnerability to machine learning attacks of optical encryption based on diffractive imaging,” Opt. Lasers Eng., vol. 125, pp. 105858, February 2020.

[37] L.N. Zhou, Y. Xiao, and W. Chen, “Image recovery through turbid water under wide distance ranges,” International Conference on Optical and Photonic Engineering (icOPEN 2019), Proceedings of SPIE, 16 – 20 July 2019, Phuket, Thailand.

[38] L.N. Zhou, Y. Xiao, and W. Chen, “Learning based holographic reconstruction through a diffuser,” PhotonIcs & Electromagnetics Research Symposium (PIERS 2019), IEEE Xplore, 17 – 20 June 2019, Rome, Italy.